ECT* workshop
23 June 2022

Resonant Shattering Flares in BHNS and NSNS mergers

Duncan Neill*, David Tsang, Hendrik van Eerten,
Geoffrey Ryan, and William G. Newton

* dn431@bath.ac.uk

Resonant Shattering Flares

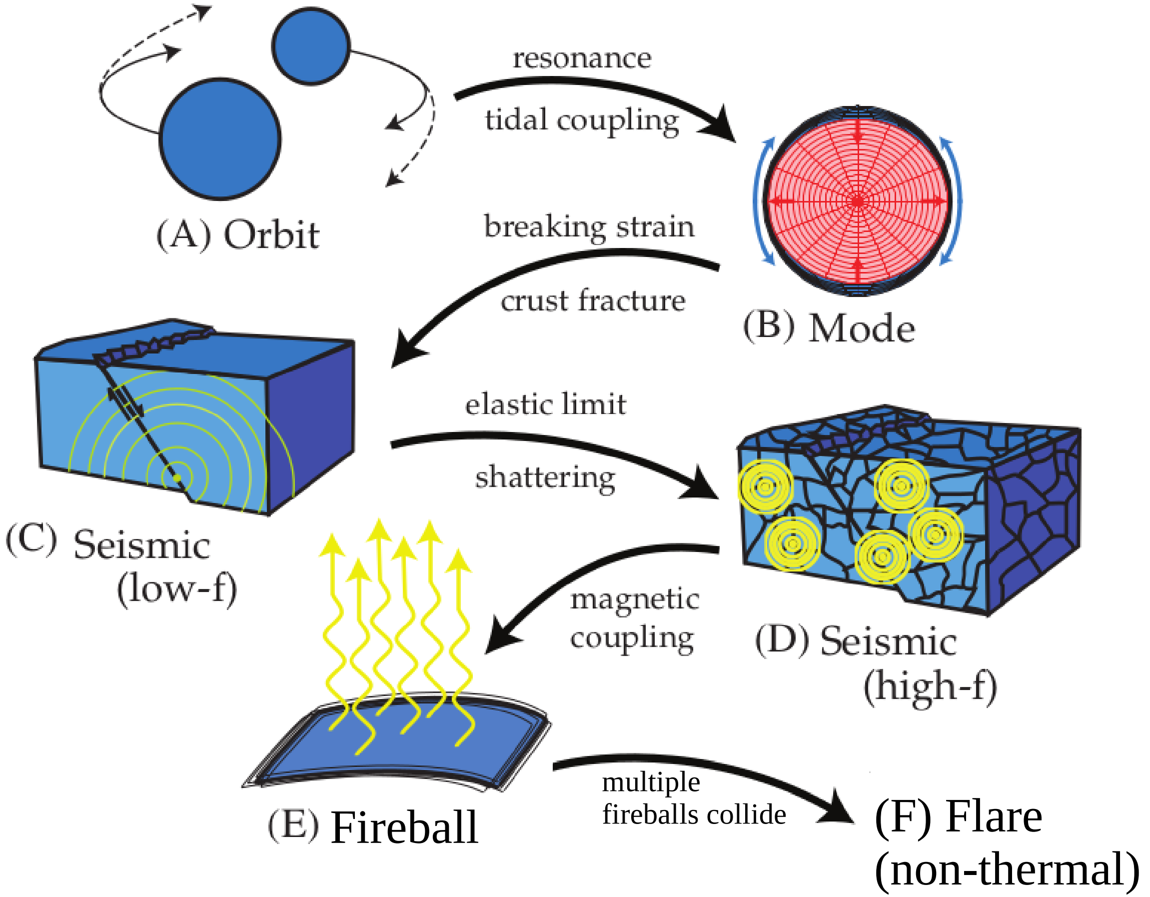

Tsang D. et al., 2012, Resonant Shattering of Neutron Star Crusts Phys. Rev. Lett., 108, 011102

Tsang D., Shattering Flares During Close Encounters of Neutron Stars, 2013, ApJ, 777, 103

Resonant Shattering Flares

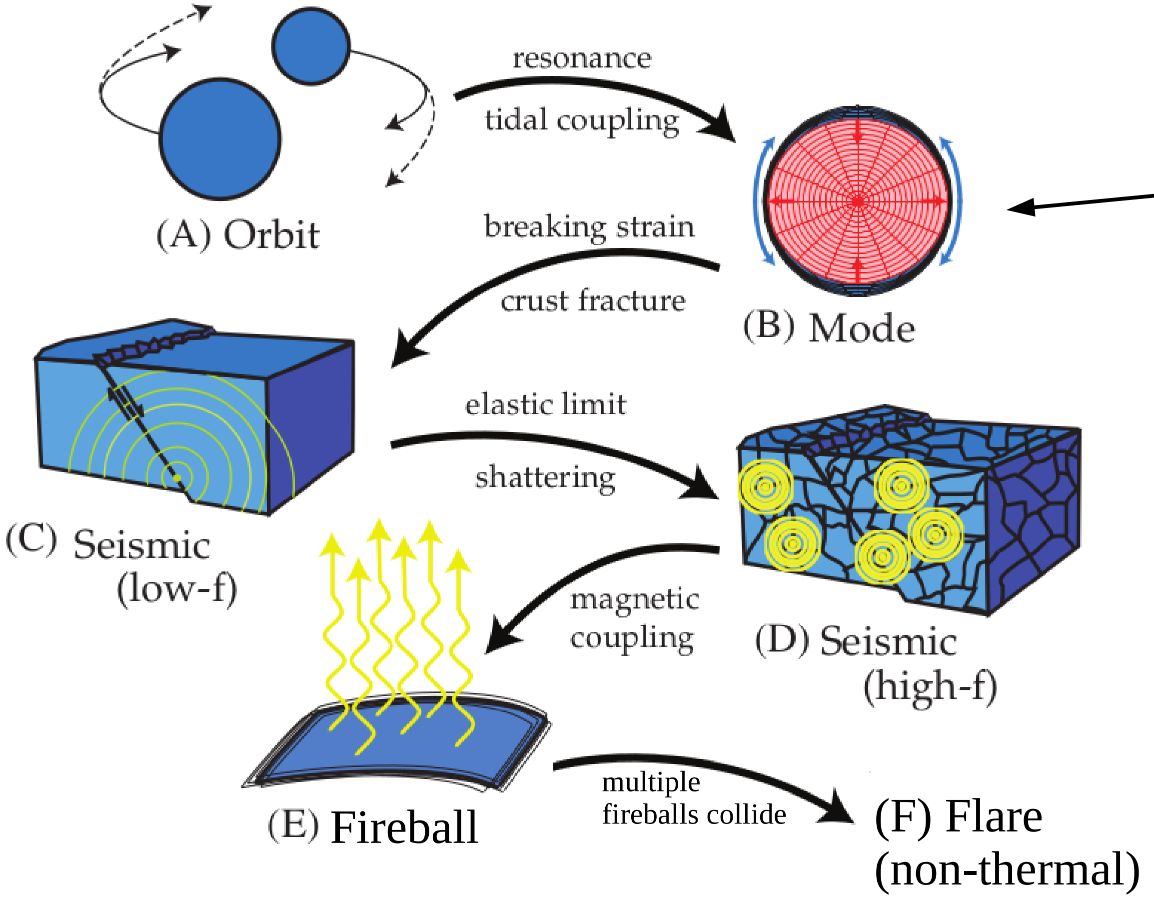

Crust-core interface mode:

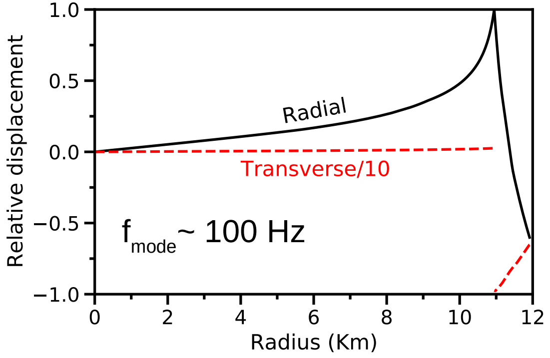

Tsang D. et al., 2012, Resonant Shattering of Neutron Star Crusts Phys. Rev. Lett., 108, 011102

Tsang D., Shattering Flares During Close Encounters of Neutron Stars, 2013, ApJ, 777, 103

Neill D., Newton W. G., Tsang D., 2021, MNRAS, 504, 1129

Resonant Shattering Flares

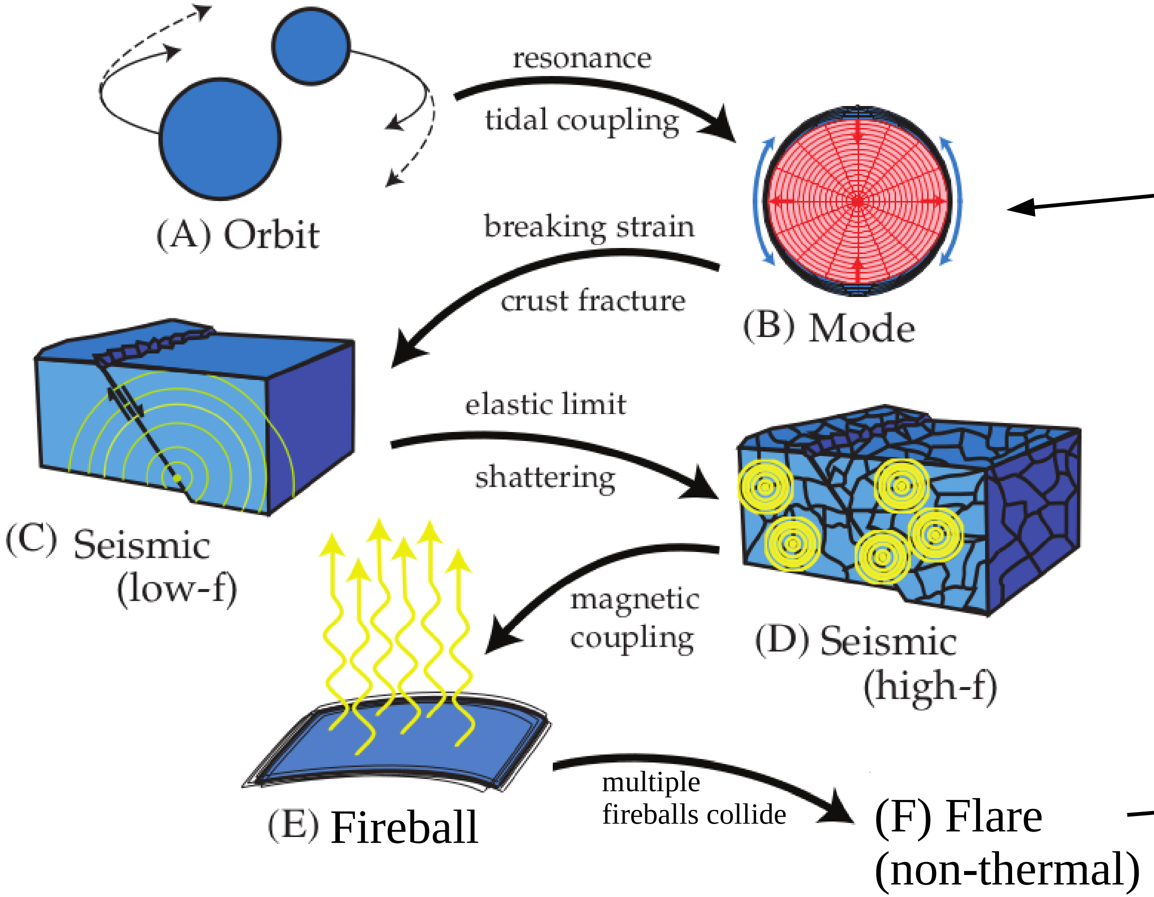

Crust-core interface mode:

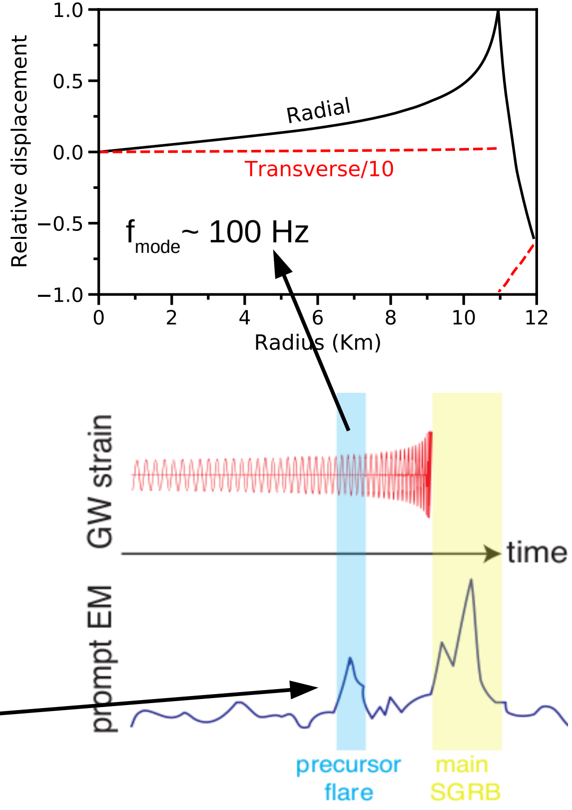

Tsang D. et al., 2012, Resonant Shattering of Neutron Star Crusts Phys. Rev. Lett., 108, 011102

Tsang D., Shattering Flares During Close Encounters of Neutron Stars, 2013, ApJ, 777, 103

Neill D., Newton W. G., Tsang D., 2021, MNRAS, 504, 1129

Bayesian parameter inference

- Injected precursor flare (RSF) detection when $f_{GW} \approx 264$ Hz (random value)
- Neutron star built from a Skyrme interaction which has the symmetry energy parameters as inputs
- Prior from causality, NICER's pulsar mass-radius constraints, and GW170817's tidal deformability (no nuclear data → high J allowed)
- We learn a lot about the combined J-L constraint, and relatively little about the NS core

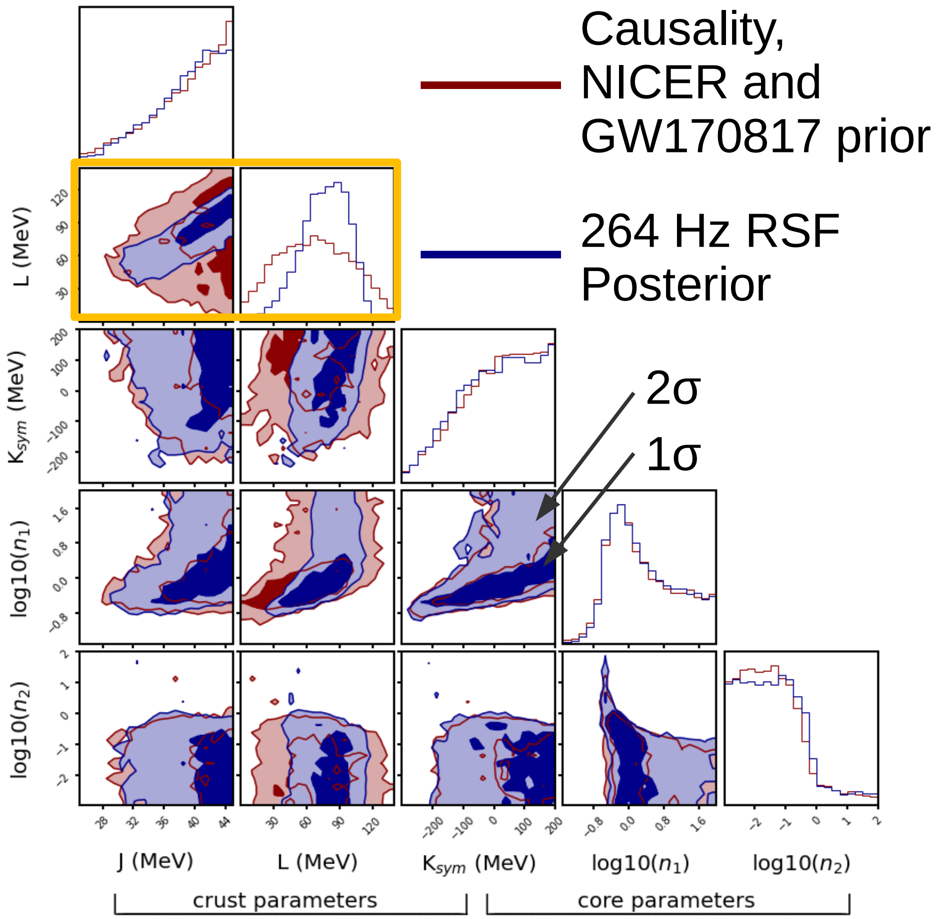

Neill D., et al., in-prep.

SGRB precursor flares

- A few percent of SGRBs are preceded by short precursors

- The cause of these flares is unclear, could they be RSFs?

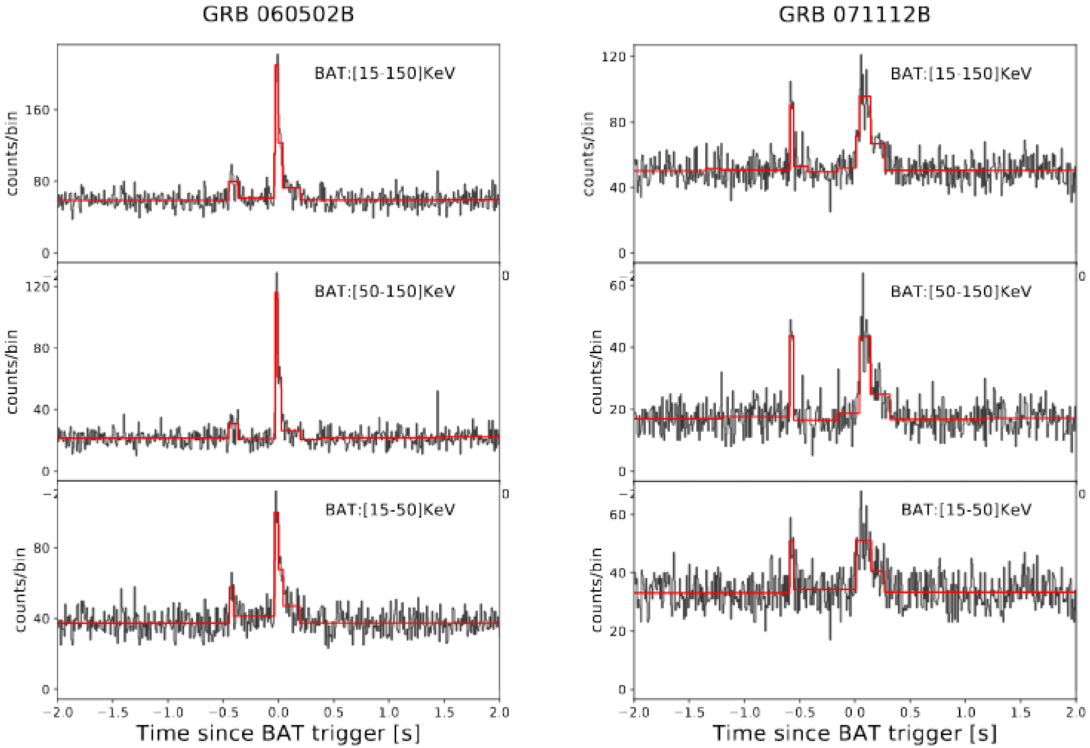

Zhong S.-Q. et al., Precursors in Short Gamma-Ray Bursts as a Possible Probe of Progenitors, 2019, ApJ, 884,25

SGRB jet model

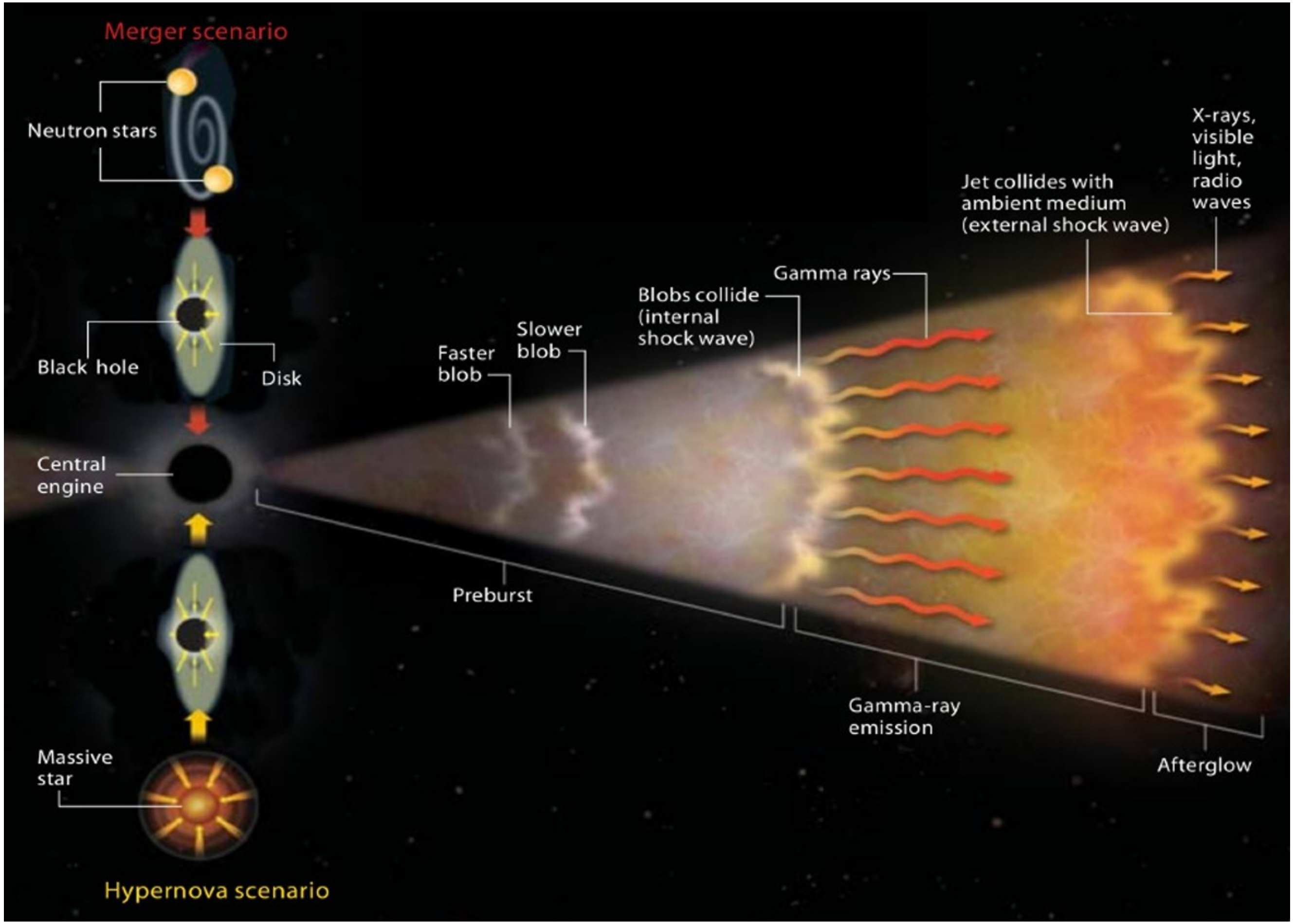

- Jet with more and less dense regions
- Dense regions collide, producing shocks
- Gamma-ray emission at shocks (synchrotron)

Piron F., 2016, CRPhy, 17, 617.

RSF shell model

- Approximately spherical shells
- Variable shell masses, so some shells are faster
- Shells collide, shocks form
- Repeated shell emission for the duration of the resonance
- Shell emission rate determined by magnetic field strength

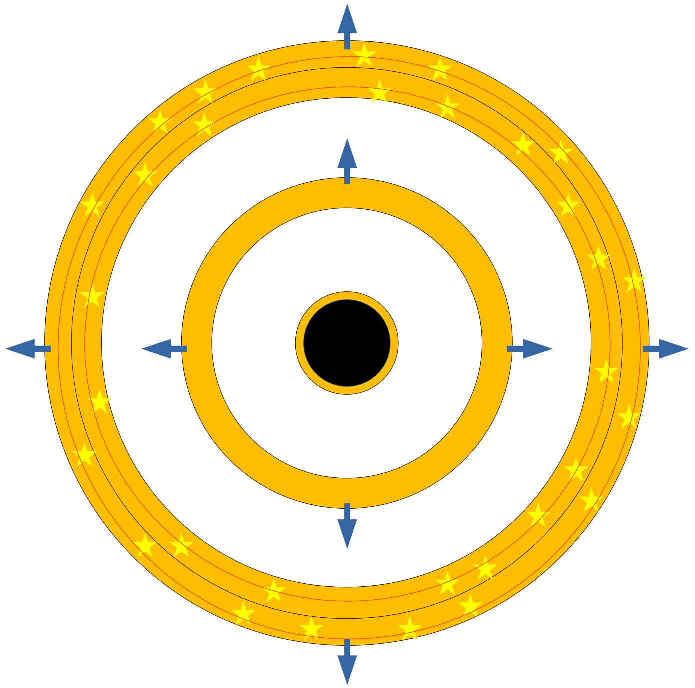

Non-thermal emission: colliding shells

- Resonance duration ≈ Flare duration
- Luminosity strongly dependent on surface magnetic field strength

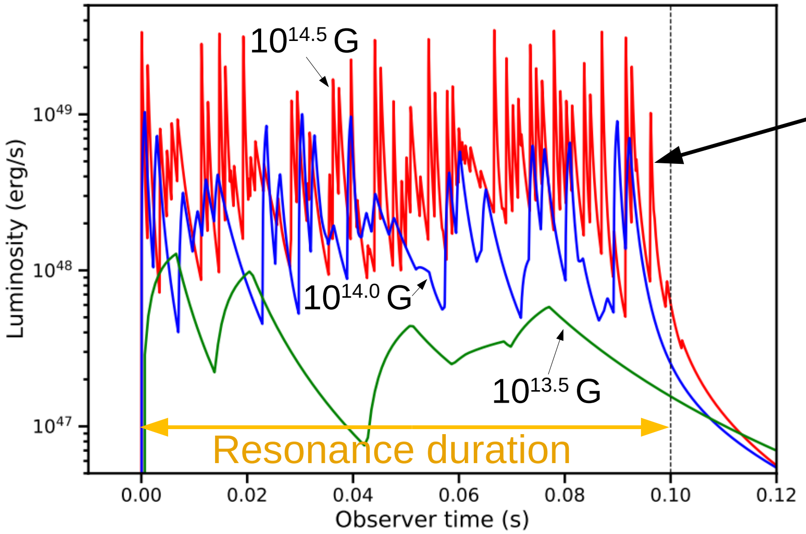

Total non-thermal luminosity (mostly gamma-rays)

Neill D., Tsang D., van Eerten H., Ryan G., Newton W. G., 2021, preprint (arXiv:2111.03686)

Non-thermal emission: colliding shells

- Resonance duration ≈ Flare duration
- Luminosity strongly dependent on surface magnetic field strength

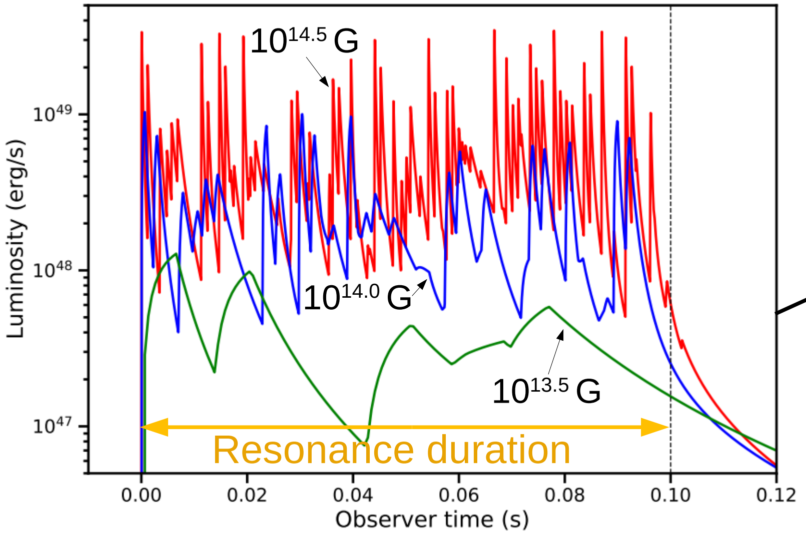

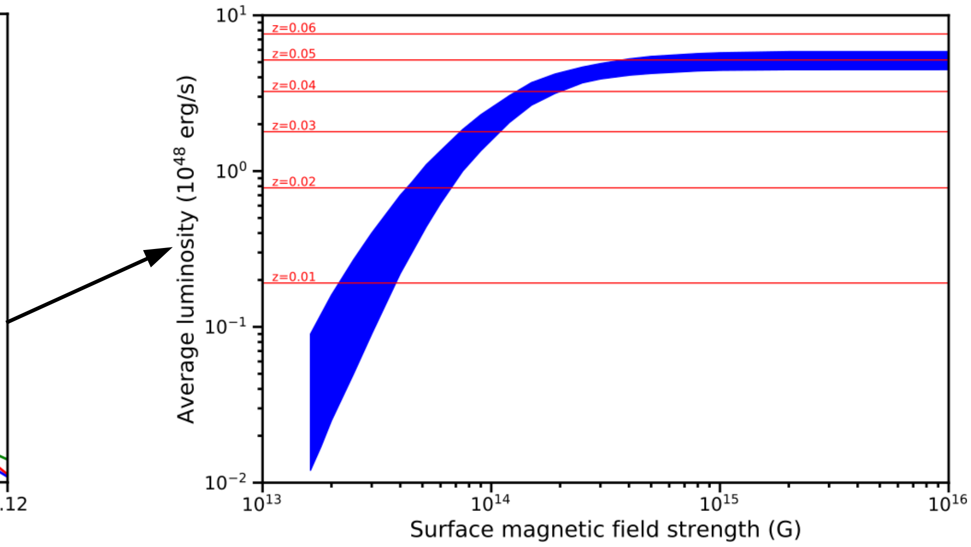

Neill D., Tsang D., van Eerten H., Ryan G., Newton W. G., 2021, preprint (arXiv:2111.03686)

NS magnetic fields

Constant dipole field

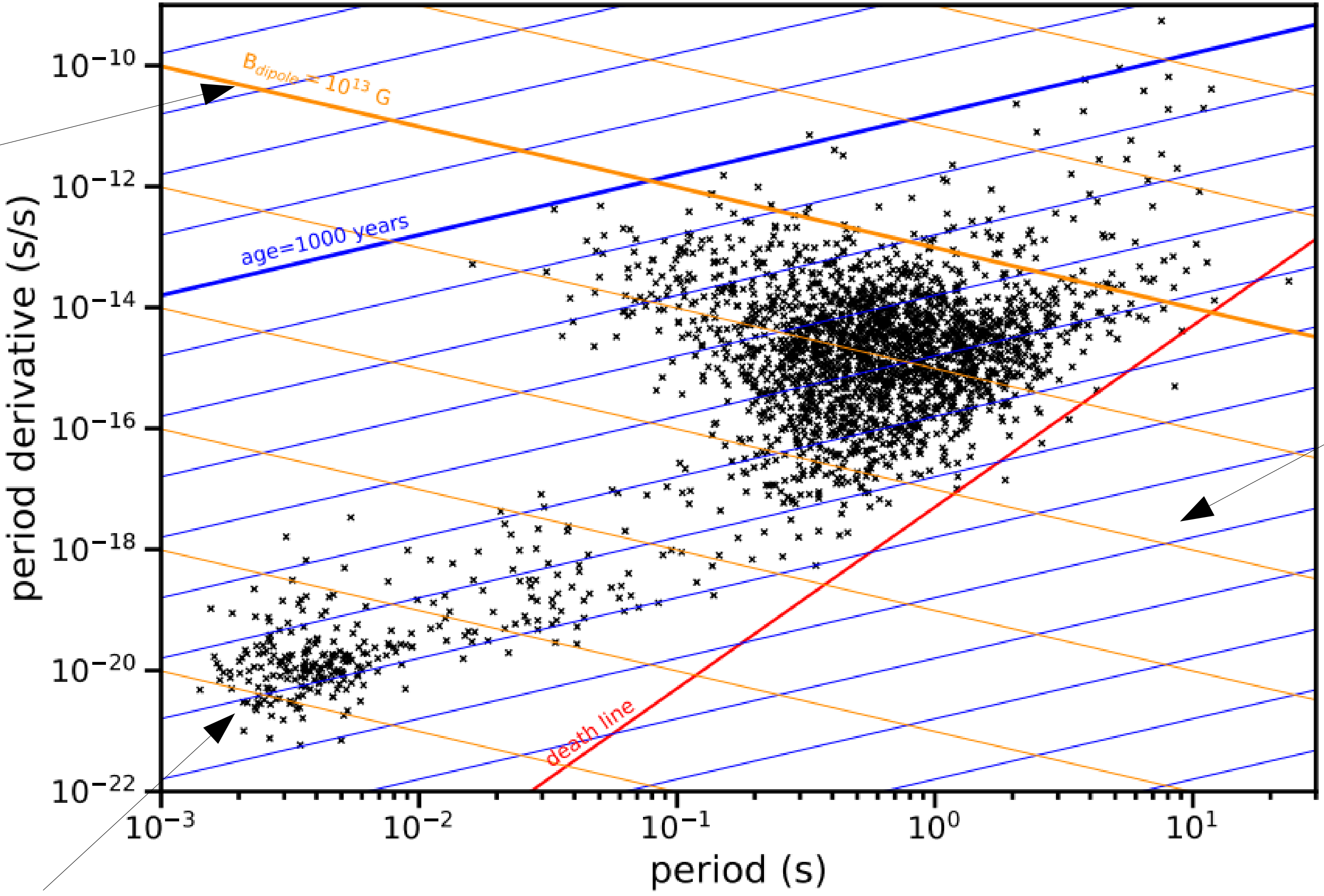

Beyond the death line, the population is unknown

MSPs: spun-up, so they are a different population

NS magnetic fields

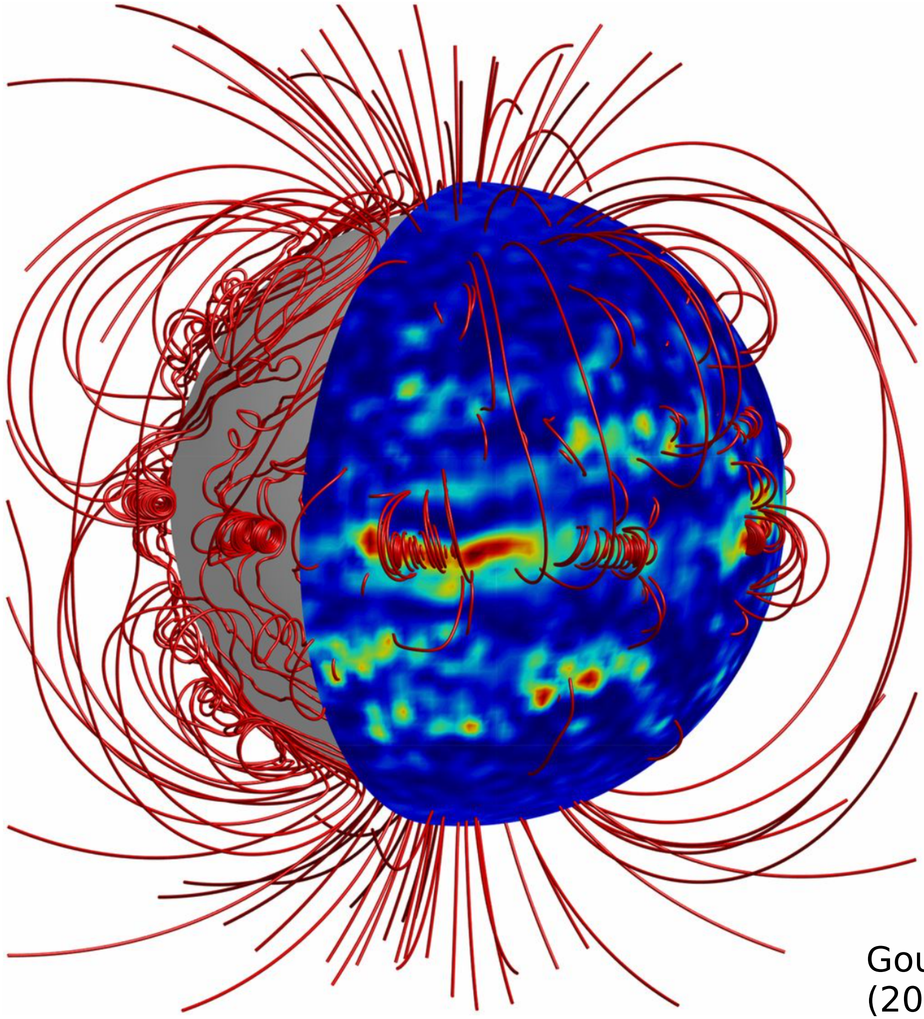

Gourgouliatos, Wood, & Hollerbach (2016) PNAS, 113, 15, 3944

NS magnetic fields

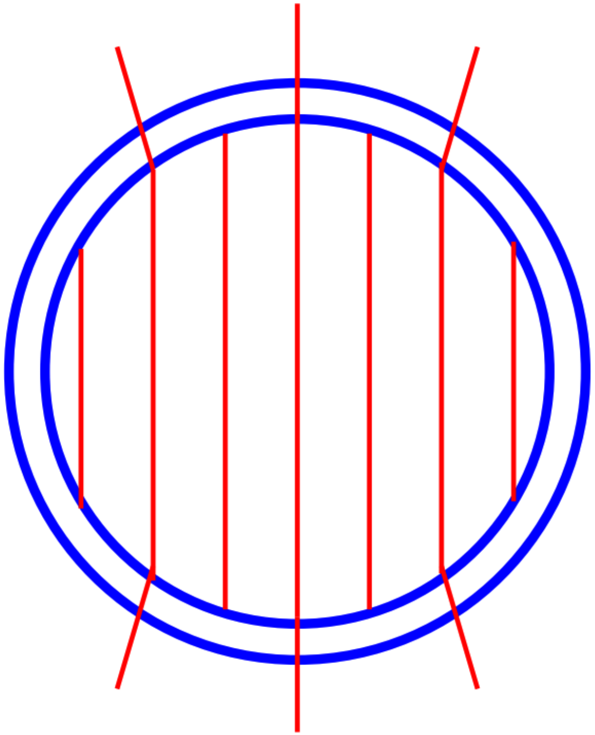

Fields that thread the superfluid core are long lived

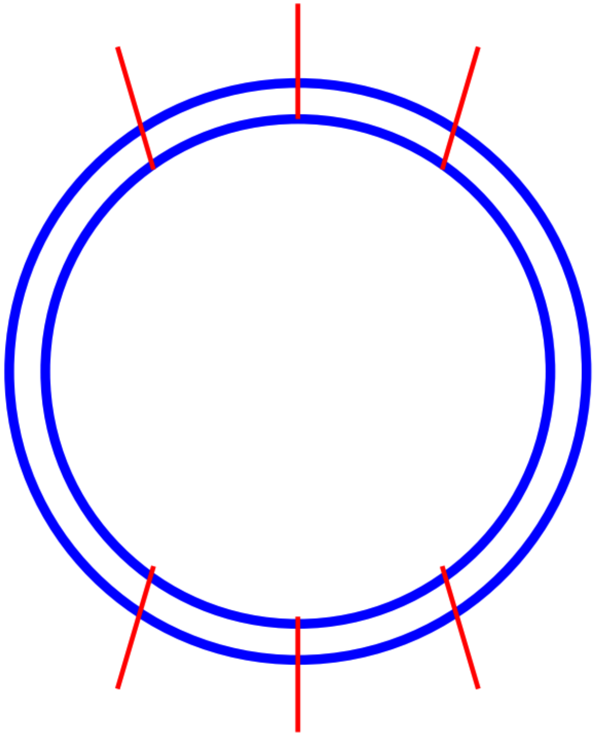

Fields that do not penetrate the core decay in < 10^6 years

Ho, Andersson & Graber (2017) PRC, 96, 065801

Konenkov & Geppert (2000) MNRAS, 313, 1, 66

Rate of RSFs

- ATNF pulsar catalogue used to estimate NS birth magnetic field distribution

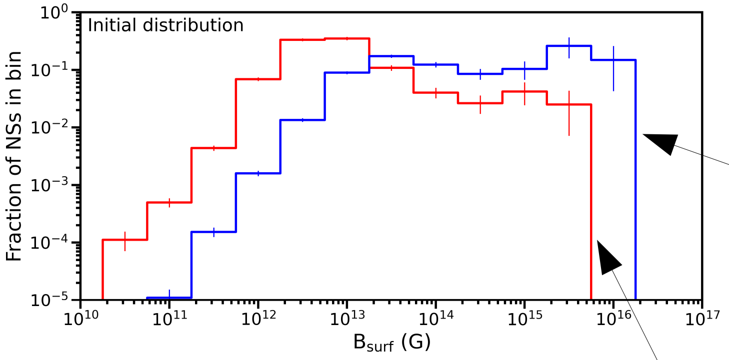

Upper bound

Lower bound

Neill D. et al., 2021, preprint (arXiv:2111.03686)

Rate of RSFs

- ATNF pulsar catalogue used to estimate NS birth magnetic field distribution
- Upper and lower bounds for magnetic field decay (which is highly uncertain)

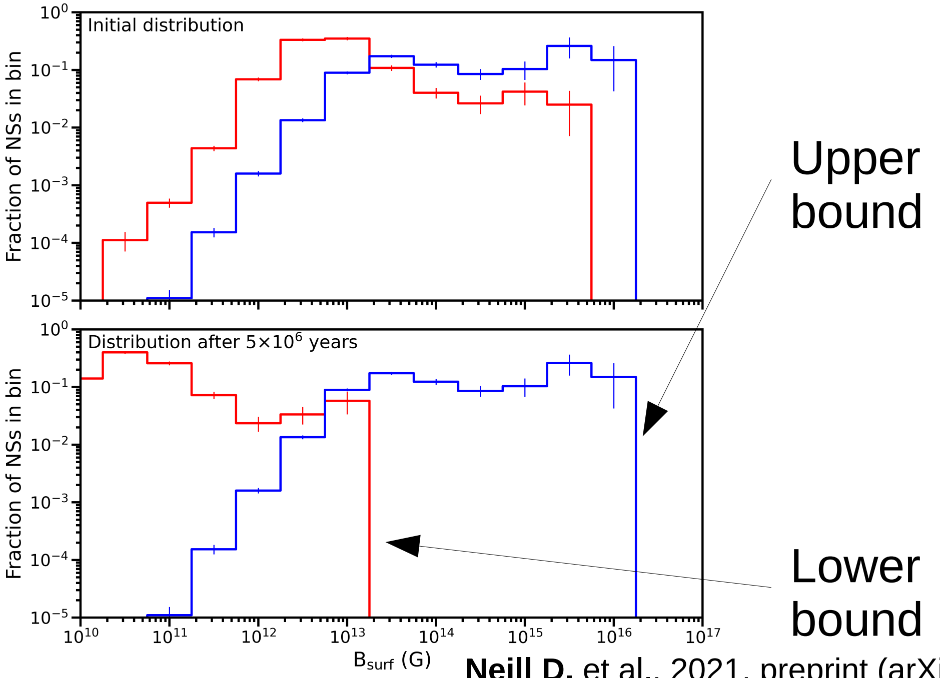

Neill D. et al., 2021, preprint (arXiv:2111.03686)

Rate of RSFs

- ATNF pulsar catalogue used to estimate NS birth magnetic field distribution
- Upper and lower bounds for magnetic field decay (which is highly uncertain)
- BPASS population synthesis model and a fit for star formation rate history used to approximate the population of BHNS mergers

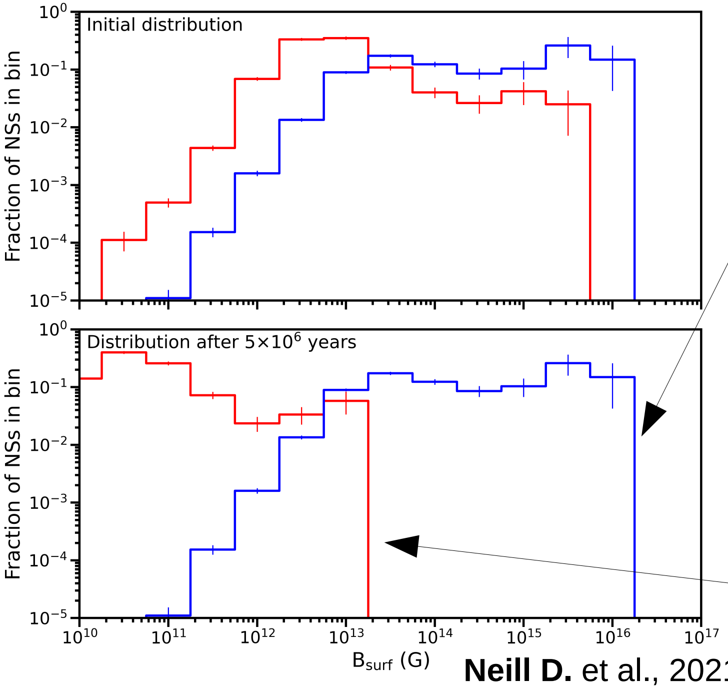

Upper bound

Lower bound

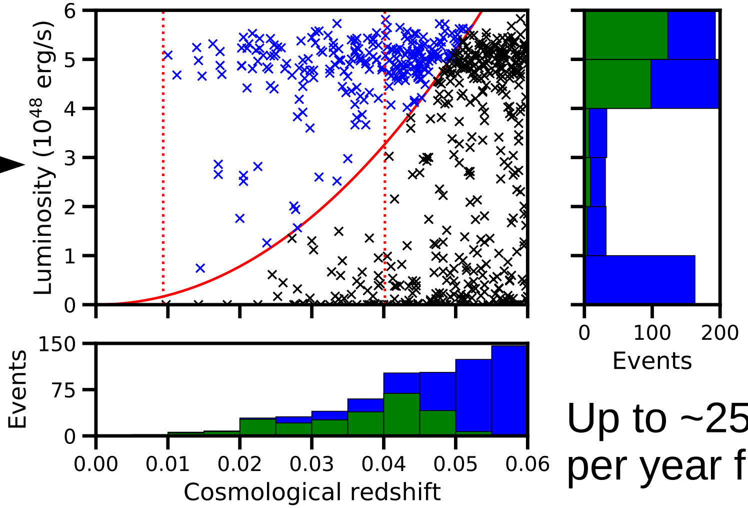

(10-year MC sample of RSF luminosities)

Up to ~25 detectable RSFs per year from NSNS

Almost all NS fields decay before merger
⟶ ~1 detectable RSF every 10000 years

Neill D. et al., 2021, preprint (arXiv:2111.03686)

Tidal disruption or resonance?

- Tidal disruption is not required for RSFs
- A significantly higher fraction of BHNS binaries may produce RSFs than SGRBs/Kilonovae

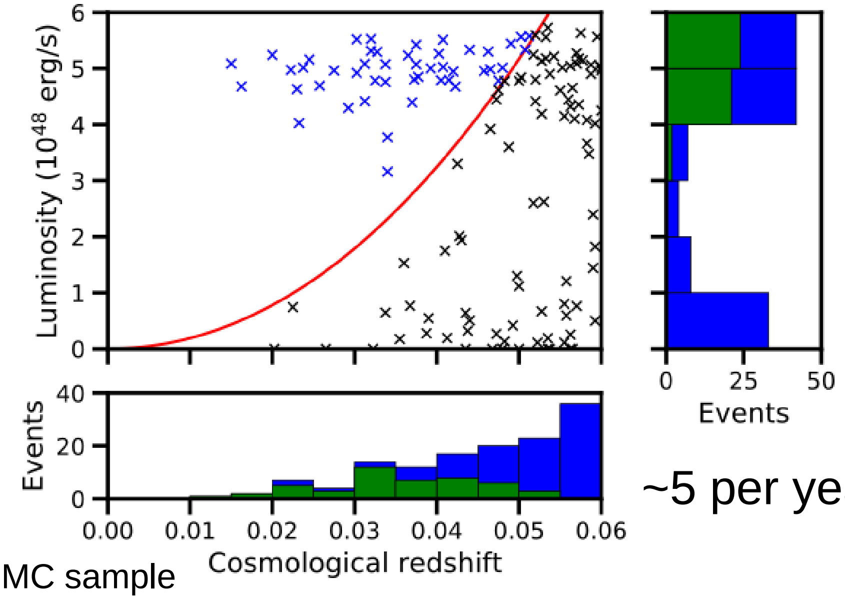

~5 per year

(10-year MC sample of RSF luminosities)

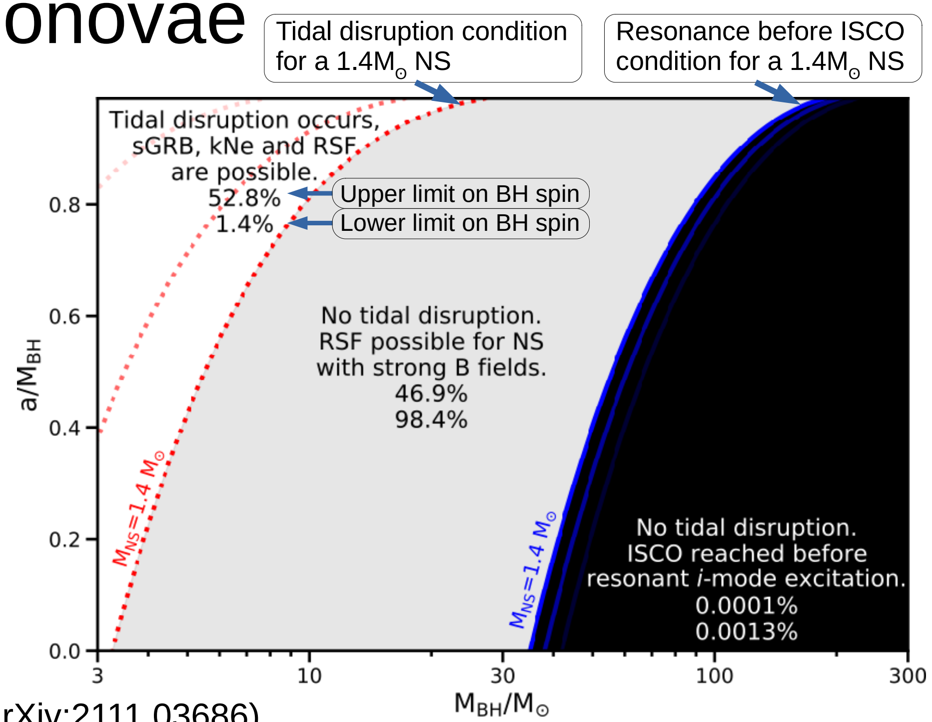

Neill D. et al., 2021, preprint (arXiv:2111.03686)

EM signals

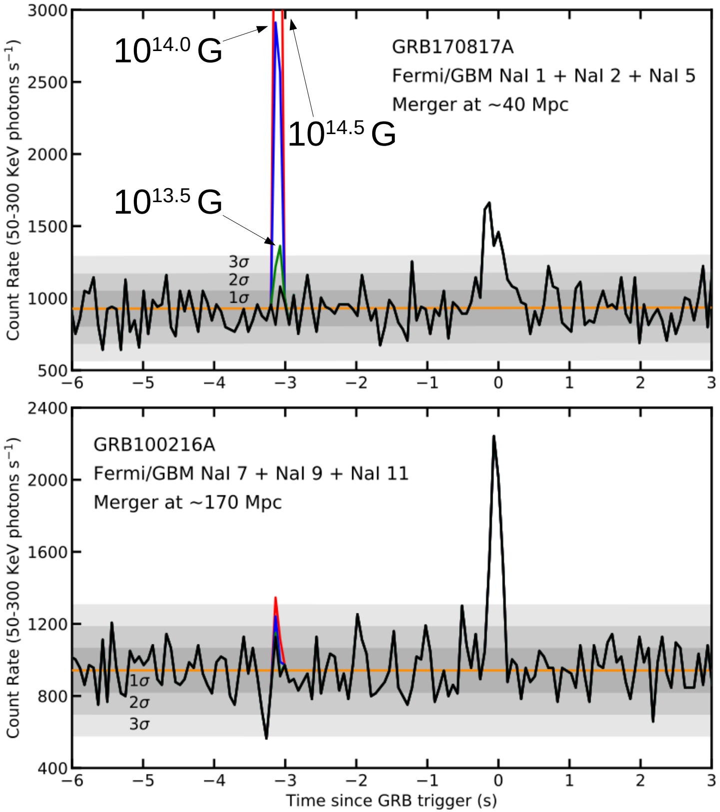

(These events are just used as examples of SGRBs, there is no evidence that either had a RSF)

Neill D. et al., 2021, preprint (arXiv:2111.03686)

EM signals

The NS involved in GW170817 likely had dipole fields below ~10^{12}G

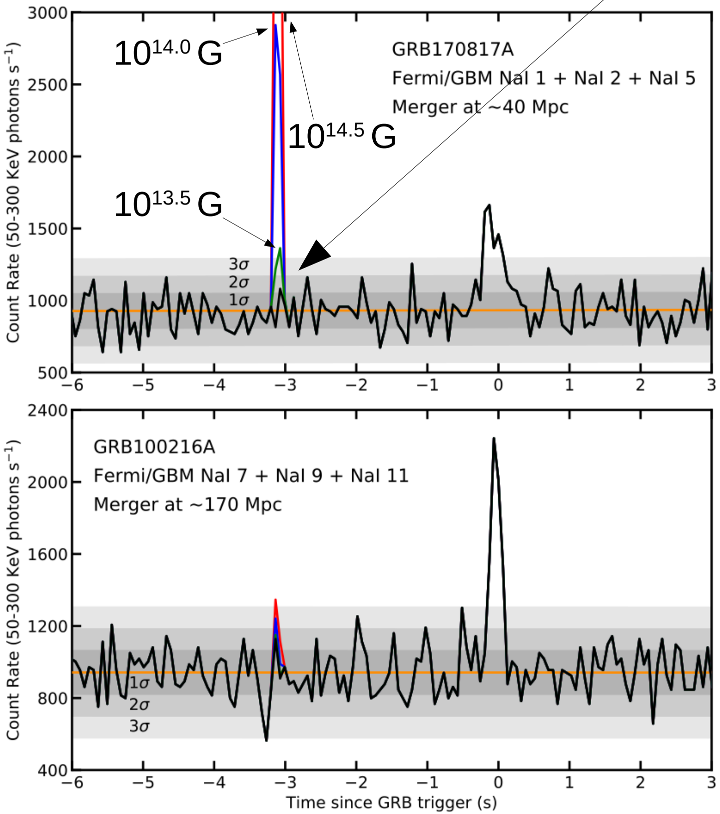

(These events are just used as examples of SGRBs, there is no evidence that either had a RSF)

Zhong S.-Q. et al., Precursors in Short Gamma-Ray Bursts as a Possible Probe of Progenitors, 2019, ApJ, 884,25

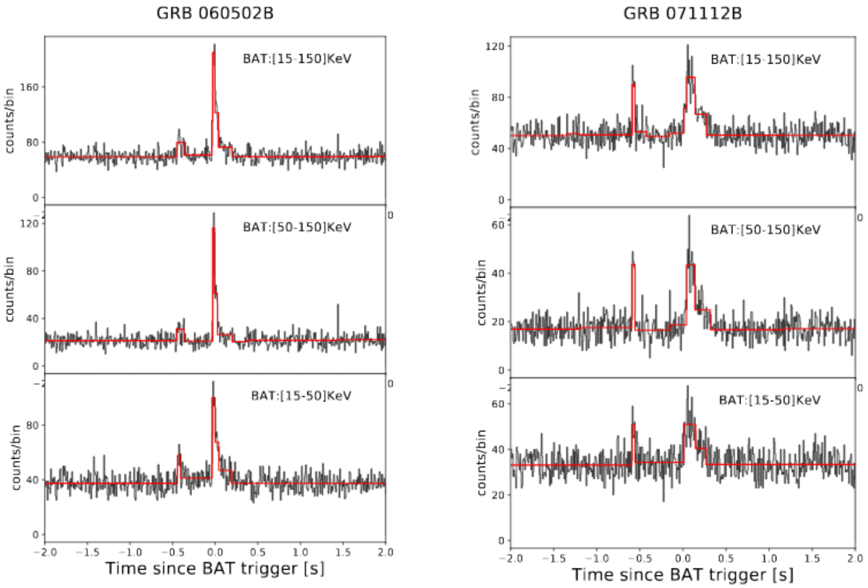

Neill D. et al., 2021, preprint (arXiv:2111.03686)

EM signals

The NS involved in GW170817 likely had dipole fields below ~10^{12}G

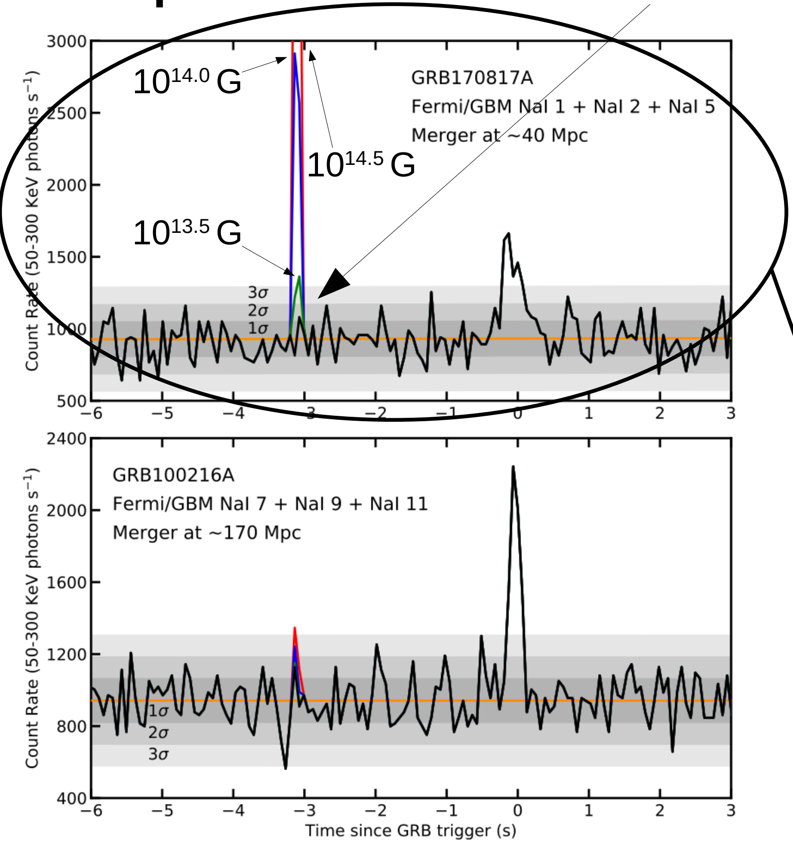

(These events are just used as examples of SGRBs, there is no evidence that either had a RSF)

Zhong S.-Q. et al., Precursors in Short Gamma-Ray Bursts as a Possible Probe of Progenitors, 2019, ApJ, 884,25

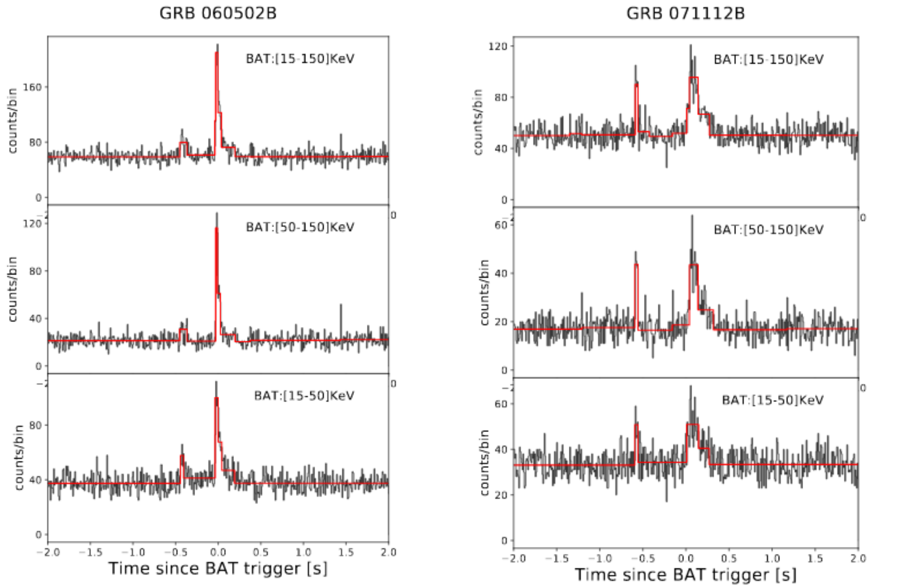

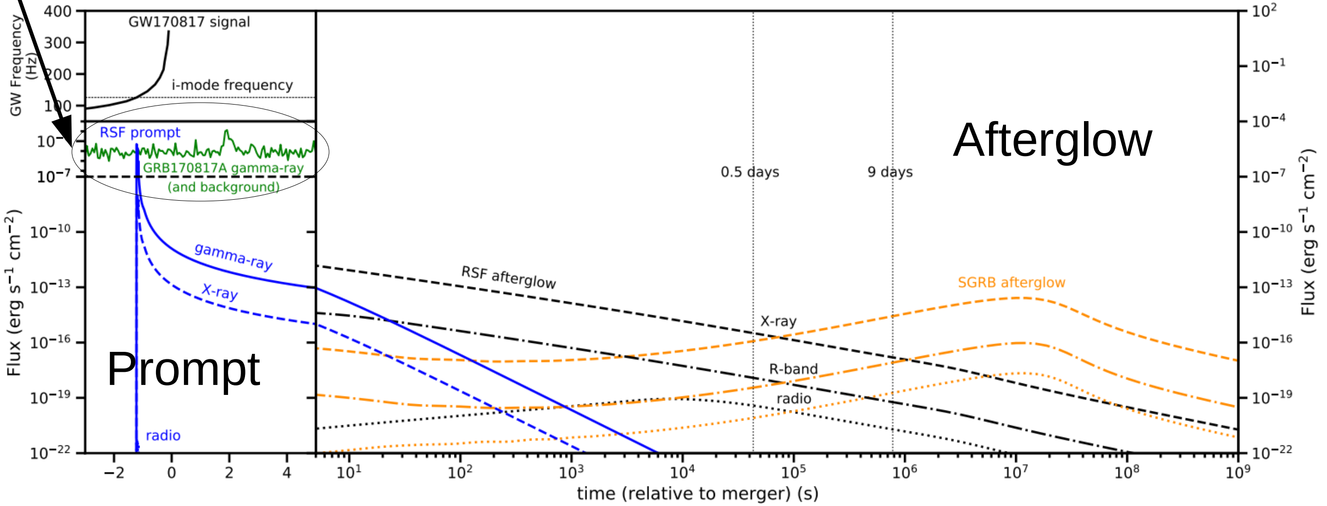

Neill D. et al., 2021, preprint (arXiv:2111.03686)

GRB211211A

- Has a kilonova
  → BHNS or NSNS merger
- Has a precursor
  → properties are consistent with our RSF calculations
- Has extended emission
  → post-merger magnetar

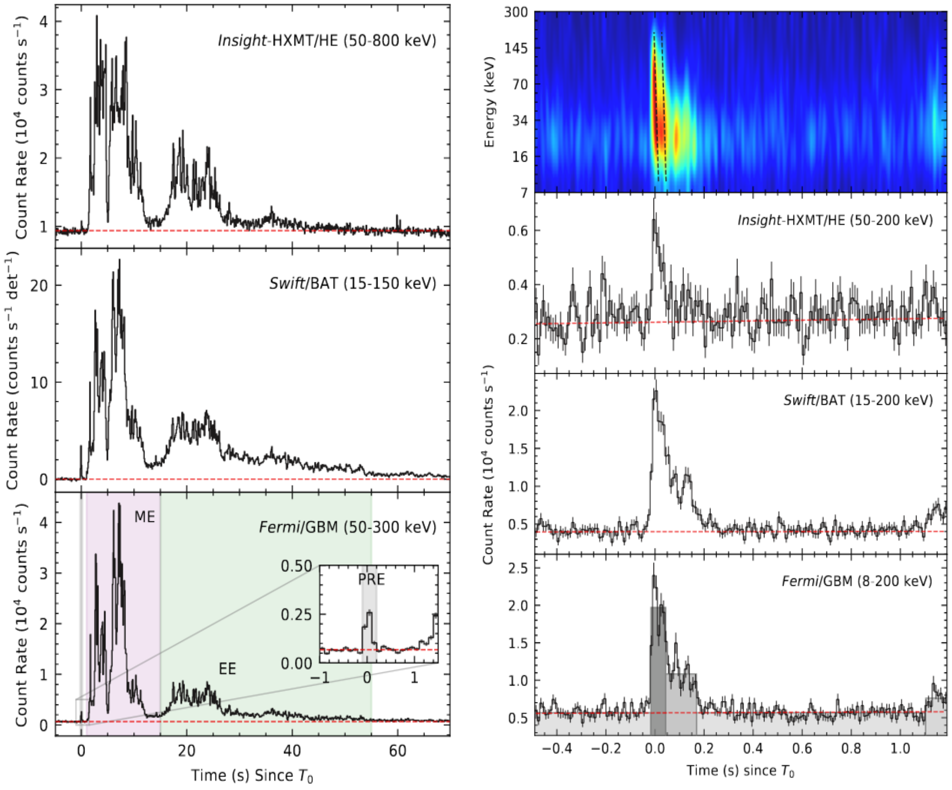

$$E_{\rm RSF} \simeq 8 \times 10^{48} {\rm erg} \ \Rightarrow B_{\rm surf} \gtrsim 10^{14.5} {\rm G}$$

Xiao S., et al., The quasi-periodically oscillating precursor of a long gamma-ray burst from a binary neutron star merger, 2022, arXiv:2205.02186

Conclusions

- Multimessenger detection of a RSF and the GW chirp from a BHNS or NSNS in-spiral would allow us to measure the i-mode frequency.
- Flare luminosity is dependent on the total surface magnetic field of the NS; magnetars can produce RSFs that are visible up to ~200 Mpc.
- Depending on the rate of NS magnetic field decay, a significant number of RSFs could be visible each year.
- RSF afterglow could be detectable if the SGRB is far off-axis, or if no SGRB is produced.
- If RSFs are precursor flares, we can make inferences of the rate at which NS magnetic fields decay. The lack of a RSF before GRB170817A implies that its progenitors had $B_{surf} < 10^{13}$G.

  - Tsang D., Read J. S., Hinderer T., Piro A. L., Bondarescu R., 2012, Phys. Rev. Lett., 108, 011102
  - **Neill D.**, Newton W. G., Tsang D., 2021, MNRAS, 504, 1129
  - **Neill D.**, Tsang D., van Eerten H., Ryan G., Newton W. G., 2021, preprint (arXiv:2111.03686)

Crust-core interface mode

Resonant ($f_{GW} \approx f_{mode}$) shortly before merger

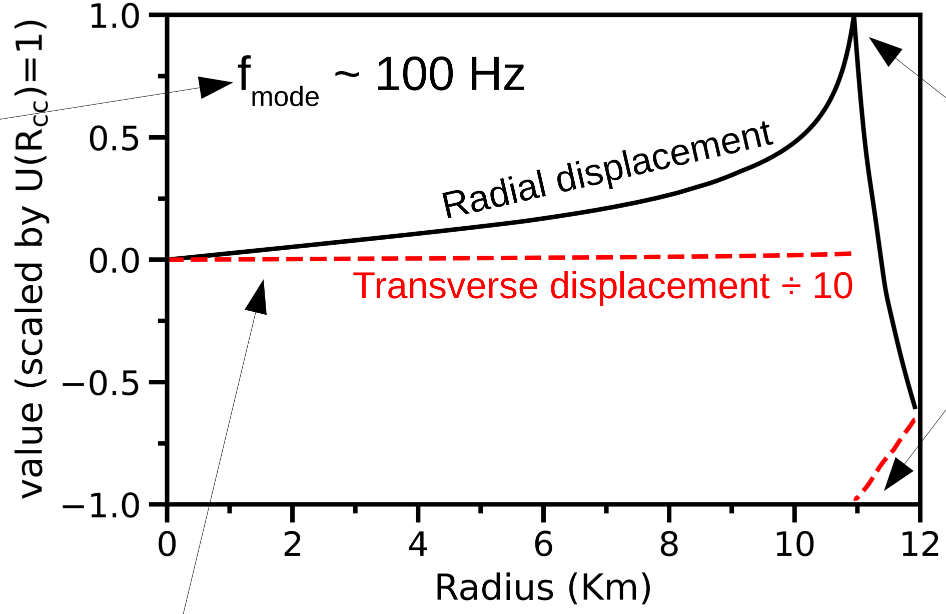

Peaks are at the crust-core boundary

Small displacements in the core

This mode has a relatively strong overlap with the tidal field

Neill D., Newton W. G., Tsang D., 2021, MNRAS, 504, 1129

How does symmetry energy affect the i-mode?

Increase in J/K_{sym} or decrease in L

Increase in E_{sym} in the crust

Higher proton fraction

Increased fraction of nucleons contained in nuclei

Increased shear modulus (and therefore shear speed)

Stronger restoring force, so a higher frequency

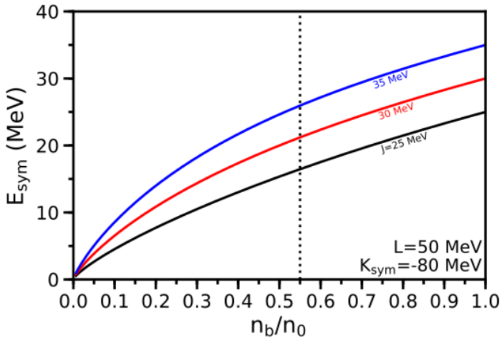

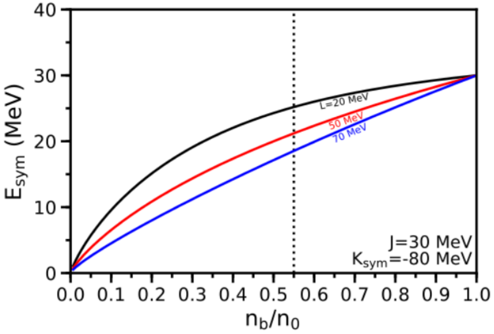

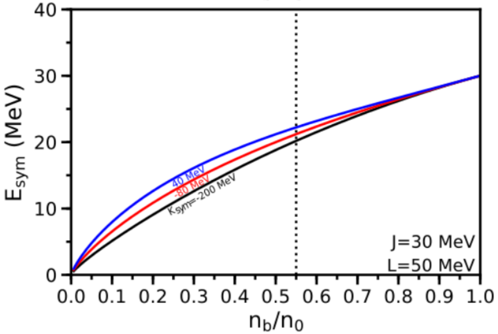

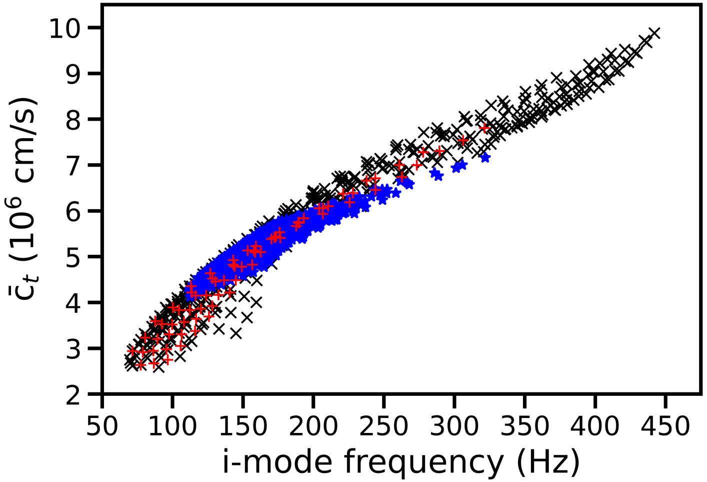

Nuclear symmetry energy

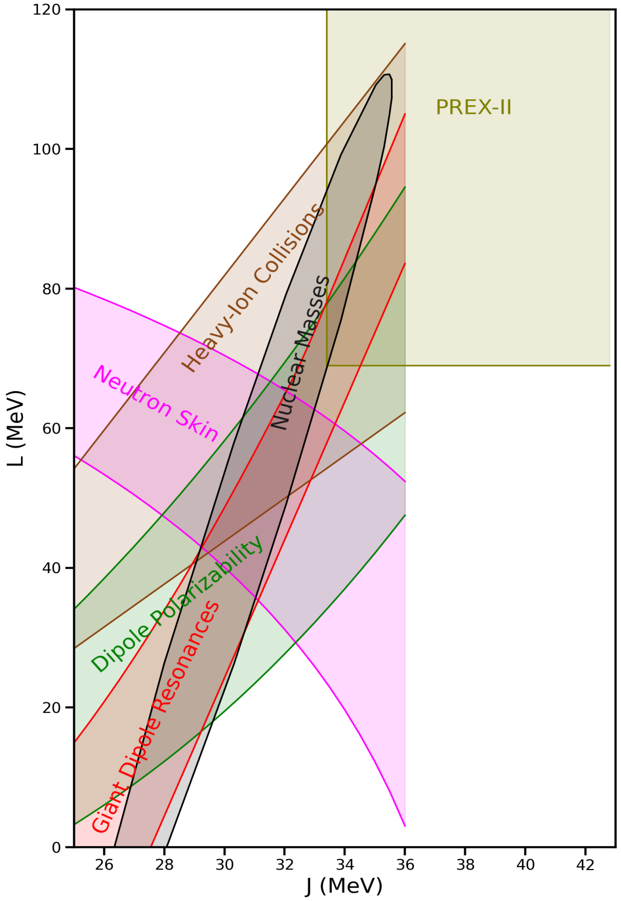

Neill D., et al., in-prep. → Based on: Lattimer J. M., Steiner A. W., 2014, European Physical Journal A, 50, 40

Nuclear symmetry energy

- RSFs provide J-L constraints competitive with collider experiments

- Constraint obtained for free when we get a multimessenger detection

GWs → RSF timing ⟶ **NS crust**

GWs → Tidal deformability → **NS core**

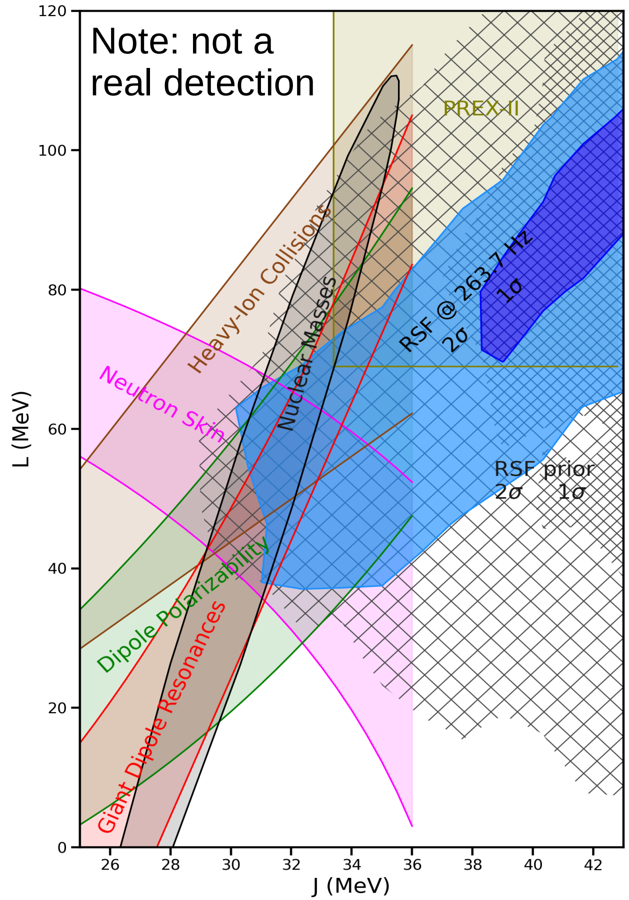

Neill D., et al., in-prep. → Based on: Lattimer J. M., Steiner A. W., 2014, European Physical Journal A, 50, 40

Neill D., Newton W. G., Tsang D.,
2021, MNRAS, 504, 1129

Initial nuclear symmetry energy parameters (J, L, K_{sym}) ranges

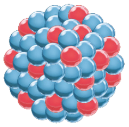

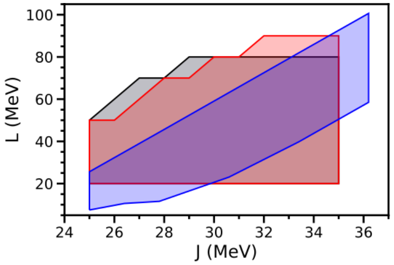

Neill D., Newton W. G., Tsang D.,
2021, MNRAS, 504, 1129

Initial nuclear symmetry energy parameters (J, L, K_{sym}) ranges

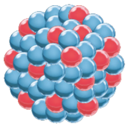

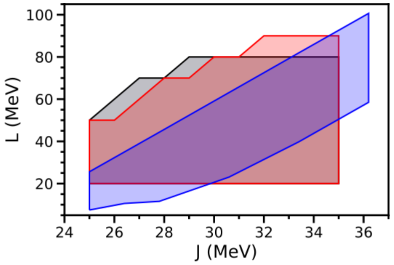

Skyrme EOS, with parameters set to produce chosen J, L, K_{sym}

Calculate NS structure and composition

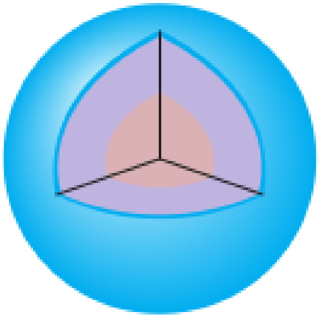

Strongly correlated with shear speed ($\bar{c}_t$), which is dependent on J,L,K_{sym}

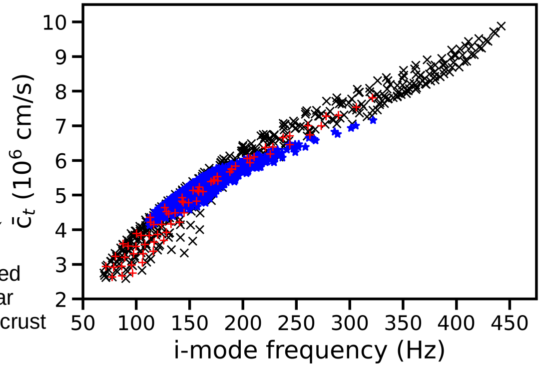

Mass-weighted average shear speed in the crust

Calculate i-mode frequency.
Calculate material properties ($\bar{c}_t$).

Neill D., Newton W. G., Tsang D., 2021, MNRAS, 504, 1129

Initial nuclear symmetry energy parameters (J, L, K_{sym}) ranges

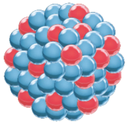

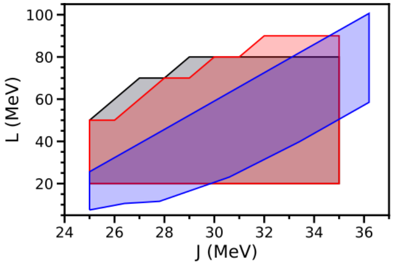

Skyrme EOS, with parameters set to produce chosen J,L,K_{sym}

Calculate NS structure and composition

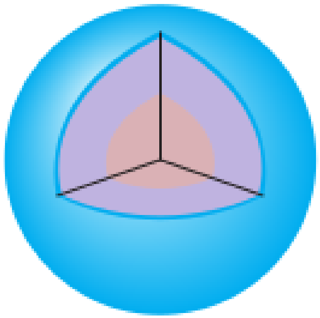

Measure frequency from multi-messenger GW+RSF detection

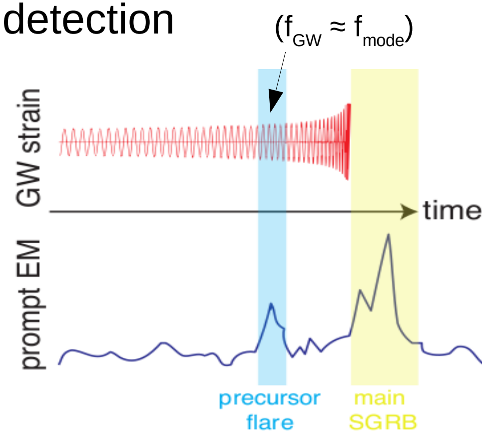

Neill D., Newton W. G., Tsang D., 2021, MNRAS, 504, 1129

Strongly correlated with shear speed ($\bar{c}_t$), which is dependent on J,L,K_{sym}

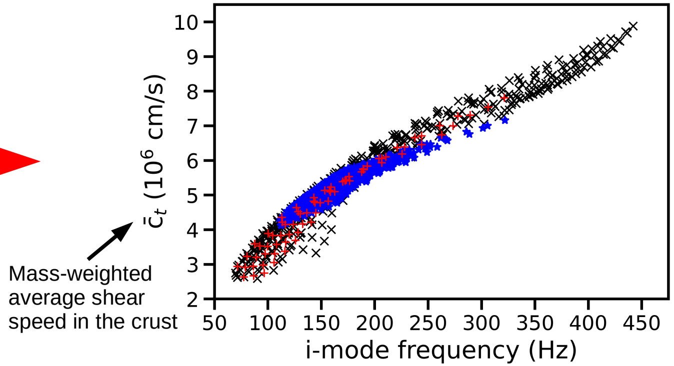

Calculate i-mode frequency.
Calculate material properties ($\bar{c}_t$).

Initial nuclear symmetry energy parameters (J, L, K_{sym}) ranges

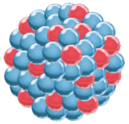

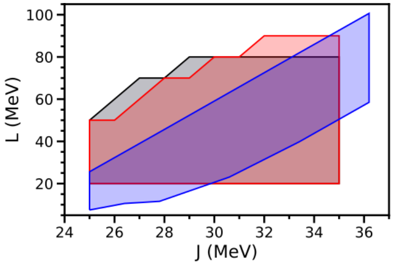

Skyrme EOS, with parameters set to produce chosen J,L,K_{sym}

Calculate NS structure and composition

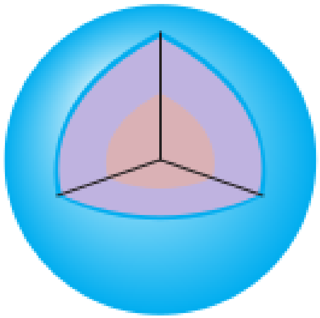

Measure frequency from multi-messenger GW+RSF detection

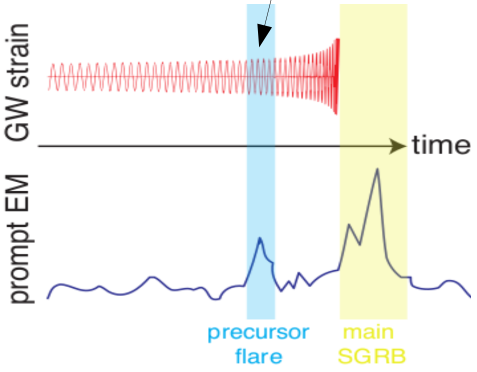

Strongly correlated with shear speed ($\bar{c}_t$), which is dependent on J,L,K_{sym}

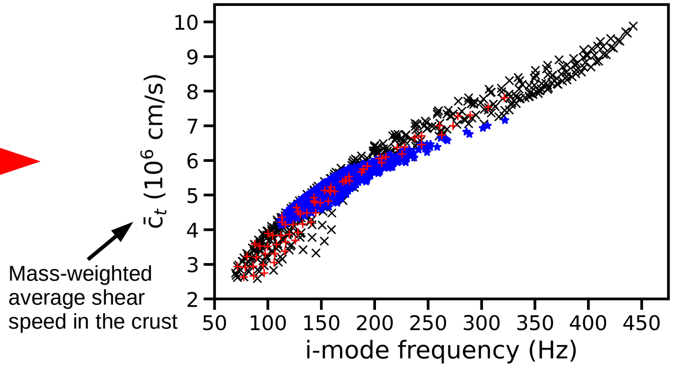

Constrain J,L,K_{sym}

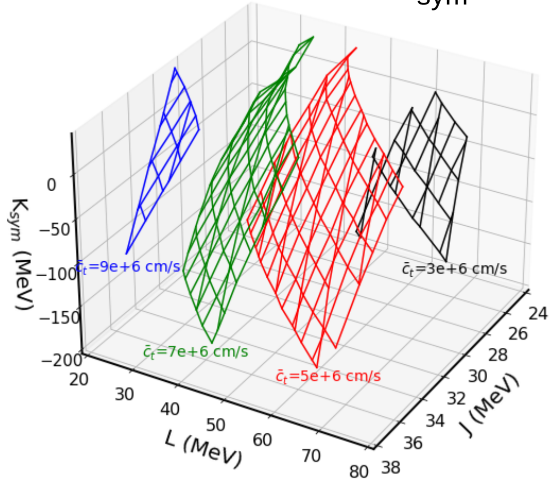

Neill D., Newton W. G., Tsang D., 2021, MNRAS, 504, 1129

Calculate i-mode frequency.
Calculate material properties ($\bar{c}_t$).

Initial nuclear symmetry energy parameters (J, L, K_{sym}) ranges

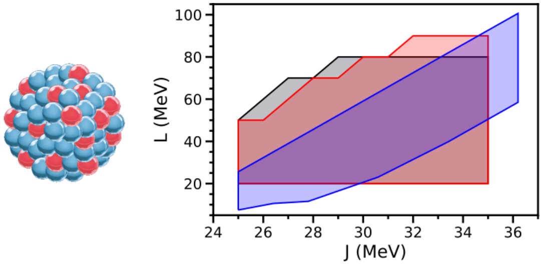

Skyrme EOS, with parameters set to produce chosen J,L,K_{sym}

Calculate NS structure and composition

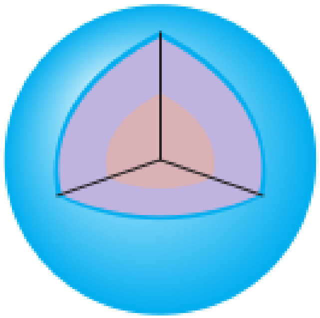

Measure frequency from multi-messenger GW+RSF detection

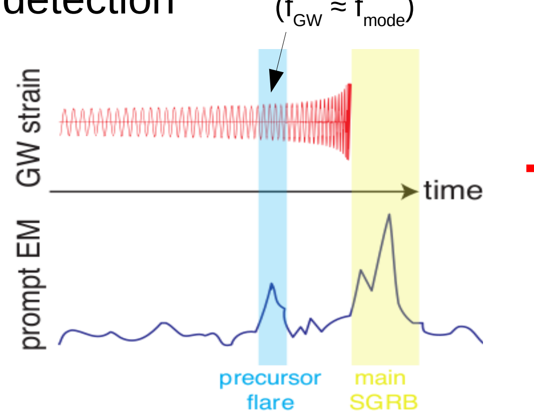

Strongly correlated with shear speed ($\bar{c}_t$), which is dependent on J,L,K_{sym}

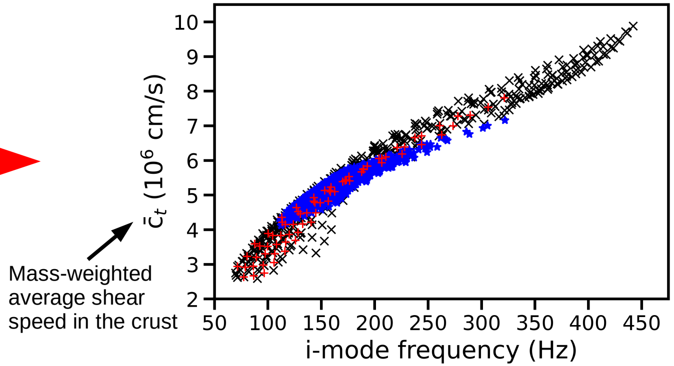

Constrain J,L,K_{sym}

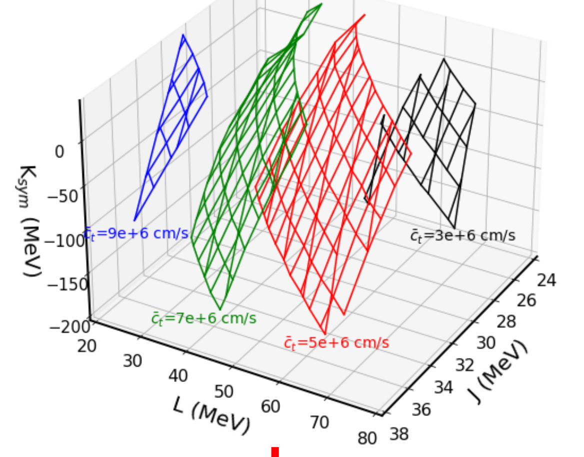

Neill D., Newton W. G., Tsang D., 2021, MNRAS, 504, 1129

Calculate i-mode frequency.
Calculate material properties ($\bar{c}_t$).

Initial nuclear symmetry energy parameters (J, L, K_{sym}) ranges

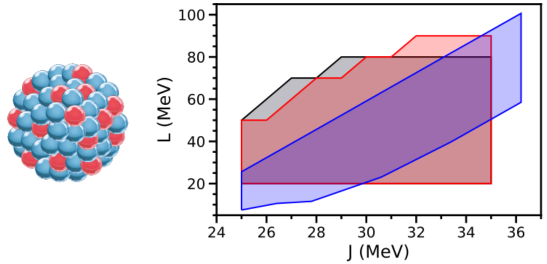

Skyrme EOS, with parameters set to produce chosen J,L,K_{sym}

Calculate NS structure and composition

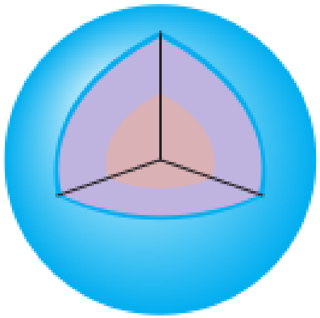

Constrain NS EOS